ON THE USE OF SPECTRAL LIBRARIES TO PERFORM SPARSE UNMIXING OF HYPERSPECTRAL DATA

Marian-Daniel Iordache, Antonio Plaza

Department of Technology of Computers and Communications, Escuela Politécnica, University of Extremadura, Cáceres, E-10071, Spain

José Bioucas-Dias

Instituto Superior Técnico Instituto de Telecomunicações Lisboa, 1049-001, Portugal

ABSTRACT

In recent years, the increasing availability of spectral libraries has opened a new path toward solving the hyperspectral unmixing problem in a semi-supervised fashion. The spectrally pure constituent materials (called *endmembers*) can be derived from a (potentially very large) spectral library and used for unmixing purposes. The advantage of this approach is that the results of the unmixing process do not depend on the availability of pure pixels in the original hyperspectral data nor on the ability of an endmember extraction algorithm to identify such endmembers. However, resulting from the fact that spectral libraries are usually very large, this approach generally results in a *sparse* solution. In this paper, we investigate the sensitivity of sparse unmixing techniques to certain characteristics of real and synthetic spectral libraries, including parameters such as mutual coherence and spectral similarity between the signatures contained in the library. Our main goal is to illustrate, via detailed experimental assessment, the potential of using spectral libraries to solve the spectral unmixing problem.

Index Terms— Hyperspectral imaging, spectral unmixing, sparse regression, spectral libraries.

1. INTRODUCTION

Spectral unmixing aims at estimating the fractional abundances of pure spectral signatures (also called *endmembers*) in each mixed pixel collected by an imaging spectrometer [1]. The linear mixing model [2] assumes that the observed (measured) spectrum of a pixel can be expressed as a linear combination of the spectra of the endmembers present in the respective pixel. It can be expressed mathematically as follows:

$$y_i = \sum_{j=1}^{q} m_{i,j}\alpha_j + n_i, \quad (1)$$

where y_i is the measured value of the reflectance at spectral band i, m_{ij} is the reflectance of the j-th endmember at spectral band i, α_j is the fractional abundance of the j-th endmember, and n_i represents the error term for the spectral band i (i.e. the noise affecting the measurement process). If we assume that the hyperspectral sensor used in data acquisition has L spectral bands, Eq. (1) can be rewritten in compact matrix form as:

$$\mathbf{y} = \mathbf{M}\boldsymbol{\alpha} + \mathbf{n}, \quad (2)$$

where $\mathbf{y}$ is an $L \times 1$ column vector (the measured spectrum of the pixel), $\mathbf{M}$ is an $L \times q$ matrix containing q pure spectral signatures (endmembers), $\boldsymbol{\alpha}$ is a $q \times 1$ vector containing the fractional abundances of the endmembers, and $\mathbf{n}$ is an $L \times 1$ vector collecting the errors affecting the measurements at each spectral band. Two constraints are usually applied to the fractional abundances collected in $\boldsymbol{\alpha}$, arising from their physical meaning: they can not be negative (the abundance non-negativity or ANC constraint) and they should sum to one (the abundance sum-to-one or ASC constraint).

In many situations, the identification of endmember signatures in the original data (e.g., by a certain algorithm developed for this purpose [3]) may be challenging due to insufficient spatial resolution, mixtures happening at different scales, and unavailability of completely pure spectral signatures in the scene. Quite opposite, the spectral unmixing problem can be tackled in semi-supervised fashion, i.e. we may look for the endmembers in a large dictionary available *a priori*, called spectral library and denoted by $\mathbf{A}$, containing p members. As a result, Eq. (2) can be rewritten as follows:

$$\mathbf{y} = \mathbf{A}\mathbf{x} + \mathbf{n} \quad (3)$$

where $\mathbf{x}$ is the new vector of fractional abundances. As the number of endmembers q is much smaller than the number p of spectra contained in $\mathbf{A}$, the vector of fractional abundances $\mathbf{x}$ is *sparse*. This characteristic of the solution is exploited by so-called sparse unmixing algorithms, which enforce it explicitly as opposed to other non-sparse algorithms which do not explicitly enforce the sparsity of the solution.

In this paper, we investigate the sensitivity of sparse unmixing techniques to certain characteristics of real and syn-

This work has been supported by the European Community's Marie Curie Research Training Networks Programme under contract MRTN-CT-2006-035927, Hyperspectral Imaging Network (HYPER-I-NET) .

thetic spectral libraries, including parameters such as mutual coherence and spectral similarity between the signatures contained in the library. The remainder of the paper is organized as follows. Section 2 presents the unmixing algorithms considered in our study. Section 3 presents our detailed experimentation, focused on comparing the unmixing results provided by those algorithms using different spectral libraries in a simulated environment (with and without enforcing the ASC and ANC constraints). Finally Section 4 concludes with some remarks and hints at plausible future research lines.

2. SPECTRAL UNMIXING ALGORITHMS

In finding sparse solutions to the unmixing problem, we would like to solve the following optimization problem:

$$(P_0): \quad \min_{\mathbf{x}} \|\mathbf{x}\|_0 \quad \text{subject to} \quad \mathbf{A}\mathbf{x} = \mathbf{y}, \tag{4}$$

where $\|\mathbf{x}\|_0$ represents the l_0 norm of $\mathbf{x}$, which simply counts the non-zero components of $\mathbf{x}$. Unfortunately, this is an NP-hard optimization problem. Under certain conditions [4, 5, 6], the l_0 norm can be replaced by the l_1 norm, leading to the convex optimization problem

$$(P_1): \quad \min_{\mathbf{x}} \|\mathbf{x}\|_1 \quad \text{subject to} \quad \mathbf{A}\mathbf{x} = \mathbf{y}. \tag{5}$$

In the presence of perturbations due to noise and modeling erros, the optimization problem (5) is very often replaced with

$$(P_1^{\delta}): \quad \min_{\mathbf{x}} \|\mathbf{x}\|_1 \ \text{ subject to } \ \|\mathbf{y} - \mathbf{A}\mathbf{x}\|_2 \leq \delta, \tag{6}$$

where δ is a majorizer for the Euclidian norm of the perturbation $\mathbf{n}$ present in the observation model $\mathbf{y} = \mathbf{A}\mathbf{x} + \mathbf{n}$, i.e., $\|\mathbf{n}\|_2 \leq \delta$.

With the above general definitions in mind, we describe next the two spectral unmixing algorithms considered in our study, namely, the classical orthogonal matching pursuit (OMP) [7], and SUnSAL [8], a novel sparse unmixing algorithm which uses variable splitting and augmented Lagrangian methods.

2.1. Orthogonal Matching Pursuit (OMP)

OMP [7], developed as an alternative to matching pursuit [9], is an iterative technique which searches, at each iteration, for the spectral signature from $\mathbf{A}$ which best explains a predetermined residual. In the first iteration, the initial residual is equal to the observed spectrum of the pixel, the vector of fractional abundances is null and the matrix of indices of selected endmembers is empty. Then, at each iteration the alforithm finds the member of $\mathbf{A}$ which is best correlated to the actual residual, adds this member to the endmembers matrix, updates the residual and computes the estimate of $\mathbf{x}$ using the selected endmembers. The algorithm finalizes when a stopping criterion is satisfied. A member from $\mathbf{A}$ can not be selected more than once, as the residual is orthogonalized with respect to the members already selected. In this work, we use OMP to solve the unconstrained problem in Eq. (6).

2.2. Sparse Unmixing via variable Splitting and Augmented Lagrangian (SUnSAL)

SUnSal [8] exploits the alternating direction method of multipliers (ADMM) [10] in a way similar to recent work [11]. The algorithm computes the solution of the following optimization problem:

$$\min_{\mathbf{x}} \frac{1}{2}\|\mathbf{A}\mathbf{x} - \mathbf{y}\|_2^2 + \lambda\|\mathbf{x}\|_1. \tag{7}$$

The objective function in (7) is composed of two terms. The first one measures the lack of fitness to the observed data $\mathbf{y}$ and the second one measures the lack of sparsity of a candidate solution. The parameter λ, called *regularization parameter*, controls the relative weight between the two terms. Problems P_1 and P_1^{δ} can be made equivalent to (7) for a suitable choice of λ. We can optionally incorporate the ANC and ASC constraints in (7). We will denote by SUnSAL+ a variant of SUnSAL which incorporates the ANC constrained.

2.3. Adapting OMP and SUnSAL to non-negative signals

By enforcing the ANC constraint, the optimization problem (5) becomes

$$(P_1^{+}): \quad \min_{\mathbf{x}} \|\mathbf{x}\|_1 \quad \text{subject to} \quad \mathbf{A}\mathbf{x} = \mathbf{y} \quad \mathbf{x} \geq 0. \tag{8}$$

Since in our problems matrix $\mathbf{A}$ contains only nonnegative entries, it can be converted into (see [5] for details)

$$(P_1^{+}): \quad \min_{\mathbf{z}} \|\mathbf{z}\|_1 \quad \text{subject to} \quad \mathbf{D}\mathbf{z} = \mathbf{y} \quad \mathbf{z} \geq \mathbf{0}, \tag{9}$$

where $\mathbf{D} \equiv \mathbf{A}\mathbf{W}^{-1}$ and $\mathbf{z} \equiv \mathbf{W}\mathbf{x}$, with $\mathbf{W} \equiv \text{diag}(\mathbf{w}^T)$, $\mathbf{w}^T \equiv \mathbf{h^T}\mathbf{A}$, and $\mathbf{h}$ a column vector such that $\mathbf{w} > \mathbf{0}$. From the writing (9), it follows that $\mathbf{h^T}\mathbf{D} = [1, \ldots, 1] \equiv \mathbf{1}^T$ and then $\mathbf{1}^T\mathbf{z} = c$, with $c = \mathbf{h^T}\mathbf{y}$. We conclude, therefore, that the problem (9) automatically enforces the equality constraint $\mathbf{1}^T\mathbf{z} = c$. For this reason, we do not impose the ASC constraint.

To take errors into account, we consider a relaxation of the optimization (9) similar to that of (6):

$$(P_1^{\delta+}): \min_{\mathbf{z}} \|\mathbf{z}\|_1 \quad \text{subject to} \quad \|\mathbf{D}\mathbf{z} - \mathbf{y}\|_2 \leq \delta \ \ \mathbf{z} \geq \mathbf{0} \tag{10}$$

Hereinafter, the variants of OMP and SUnSAL dedicated to solve the optimization (10) will be denoted by OMP+D and SUnSAL+D, respectively.

3. RESULTS IN SIMULATED ENVIRONMENT

In our experiments, we used seven spectral libraries: a hypothetical one, generated as a collection of spectra containing

i.i.d. Gaussian entries, and six libraries assembled using real signatures from the U.S. Geological Survey (USGS)[1] and the NASA Jet Propulsion Laboratory's Advanced Spaceborne Thermal Emission and Reflection Radiometer (ASTER)[2] spectral libraries. The libraries, denoted by $\mathbf{A}_1 \dots \mathbf{A}_7$, were built as follows. $\mathbf{A}_1$ contains 498 spectral signatures selected from the USGS library. $\mathbf{A}_2$ is a subset of $\mathbf{A}_1$ obtained by retaining only the signatures which sufficiently differentiate between them (i.e. with spectral angle greater or equal than three degrees). $\mathbf{A}_3$ is a subset of $\mathbf{A}_1$ obtained in the same way as $\mathbf{A}_2$, but enforcing spectral angle greater or equal than six degrees. $\mathbf{A}_4$ is a collection of 500 spectral signatures extracted from the ASTER library. $\mathbf{A}_5$ and $\mathbf{A}_6$ are subsets of $\mathbf{A}_4$ generated in similar fashion to $\mathbf{A}_2$ and $\mathbf{A}_3$. Finally, $\mathbf{A}_7$ contains i.i.d. Gaussian entries. In order to get sparsest solutions, the *mutual coherence* [12] of the spectral library $\mu(\mathbf{A})$ should be as small as possible. This figure is shown in Table 1 for all libraries along with the number of signatures, the wavelength range, and the number of signatures with angles $s \leq 5^\circ$ and with angles in the interval $5^\circ \leq s \leq 10^\circ$.

Table 1. Internal characteristics of the libraries.

Spectral library	$\mathbf{A}_1$	$\mathbf{A}_2$	$\mathbf{A}_3$	$\mathbf{A}_4$	$\mathbf{A}_5$	$\mathbf{A}_6$	$\mathbf{A}_7$
Description	USGS	USGS pruned 3°	USGS pruned 6°	ASTER	ASTER pruned 3°	ASTER pruned 6°	i.i.d. Gaussian
Number of spectra	498	342	159	500	449	385	448
Minimum wavelength (w_{min}) in μm	0.4	0.4	0.4	3	3	3	-
Maximum wavelength (w_{max}) in μm	2.5	2.5	2.5	12	12	12	-
Mutual coherence $\mu(\mathbf{A})$	0.99998	0.9986	0.9945	1	0.9986	0.9944	0.2822
Spectral angle $s \leq 5^\circ$	303	144	0	92	41	0	0
Spectral angle $5^\circ \leq s \leq 10^\circ$	140	136	98	184	132	109	0

From Table 1, it can be seen that the considered libraries are highly coherent, which imposes a very low bound on the sparsity of the solution. Even pruning the libraries does not improve the mutual coherence significantly. This difficulty is attenuated by the highly sparse mixtures we typically have in hyperspectral applications. Library $\mathbf{A}_7$ has the lowest mutual coherence. We then foresee that this library yields the best unmixing results. With these observations in mind, the considered algorithms were tested both in a noiseless and in a a noisy environment. Since the perturbations in the linear mixing model are mostly modeling erros, thus, highly corrected, we generate the noise from low-pass filtering i.i.d. Gaussian random samples using a normalized cut-off frequency of $5\pi/L$. The signal-to-noise ratio (SNR $\equiv \|\mathbf{Ax}\|_2^2 / \|\mathbf{n}\|_2^2$) was set to 30dB. We considered five sparsity levels (or *cardinalities*) k of the mixtures: 1, 5, 10, 15 and 20. For every possible combination of library, noise and cardinality, we generated 100 samples, with the fractional abundances following a Dirichlet distribution. The quality of the reconstruction of a spectral mixture was measured using the reconstruction SNR: RSNR $\equiv E[\|\mathbf{x}\|_2^2]/E[\|\mathbf{x}-\hat{\mathbf{x}}\|_2^2]$, measured in dBs: RSNR(dB) $\equiv 10\log_{10}$(RSNR). The parameters used in the tests were hand tuned to near optimal performance, by running the considered algorithms for large sets of possible values of the parameters on test data sets containing a small number of samples (5) corresponding to every possible combination. As a general observation after completing this task, it can be said that the parameters used for SUnSAL and its variants, for a certain level of noise, exhibit very small variations compared to the ones used for OMP and OMP+D (which require fine-tuning). This means that, in a real scenario, the probability to find near-optimal parameters for the sparse technique is much higher than the one corresponding to the non-sparse technique.

Fig. 1 plots RSNR(dB) for all the methods and libraries, both for the observations affected and not affected by noise. Because $\mathbf{A}_7$ contains negative entries, the curves for SUnSAL+D and OMP+D obtained with library $\mathbf{A}_7$ were disregarded. From the results plotted in Fig. 1, we highlight the following aspects:

a) the values RSNR tend to decrease as k increases and as the minimum spectral angle decreases. This is more visible in the presence of noise;

b) in the absence of noise, SUnSAL+D produces values of RSNR larger that 30dB for $k \leq 20$, allowing a high quality unmixing. SUnSAL+, with RSNR larger that 10 dBs for most of the cases also ensures useful unmixings. Generally, OMP performs better than OMP+D for $k = 1$, but both methods yield low values of RSNR for $k \geq 10$, except for library $\mathbf{A}_7$;

c) in the presence of noise, the values of RSNR are, as expected, lower than in the absence of noise. In general terms, SUnSAL yields close to the best performance. Note that, for $\mathbf{A}_1$ and $\mathbf{A}_4$, which are the most coherent libraries, leading to the most difficult unmixing problem, the sparse technique, in all variants, outruns the non-sparse one, both in noiseless and noisy environment. We would say that unmixing is possible for $k \leq 10$. For larger values of k, the value of RSNR approaches 0dBs, situation in which the unmixing is very poor.

4. CONCLUSIONS

This paper analized the influence of the internal characteristics of spectral libraries on the accuracy of (semi-supervised) sparse unmixing algorithms. Two relevant indicators were inspected: the mutual coherence of the library and the spectral dissimilarity of the signatures contained in the library. Our experiments indicate that pruning the libraries (by enforcing a minimum spectral angle between the signatures), although increasing very little the mutual coherence of real libraries, leads to improvements in the sparse unmixing algorithms in noisy environments. Further experiments should be conducted with real hyperspectral data sets in order to generalize the aforementioned observations to practical hyperspectral analysis scenarios.

[1] Available online: http://speclab.cr.usgs.gov/spectral-lib.html

[2] Available online: http://speclib.jpl.nasa.gov

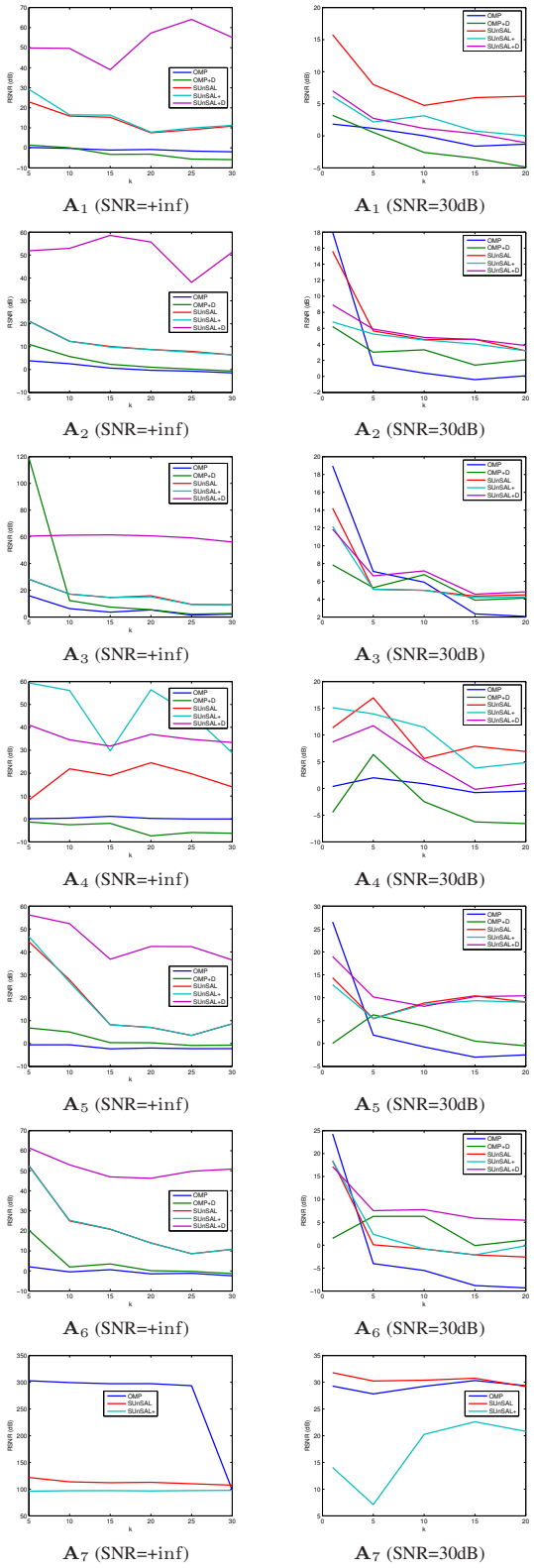

Fig. 1. Plots of the RSNR values obtained for the different methods applied to the simulated data in noiseless (SNR=+inf) and noisy (SNR=30dB) environments.

5. REFERENCES

[1] N. Keshava and J. F. Mustard, "Spectral unmixing," *IEEE Signal Processing Magazine*, vol. 19, no. 1, pp. 44–57, 2002.

[2] J. B. Adams, M. O. Smith, and P. E. Johnson, "Spectral mixture modeling: a new analysis of rock and soil types at the Viking Lander 1 site," *Journal of Geophysical Research*, vol. 91, pp. 8098–8112, 1986.

[3] A. Plaza, P. Martinez, R. Perez, and J. Plaza, "A quantitative and comparative analysis of endmember extraction algorithms from hyperspectral data," *IEEE Transactions on Geoscience and Remote Sensing*, vol. 42, no. 3, pp. 650–663, 2004.

[4] E. Candès and T. Tao, "Near-optimal signal recovery from random projections: universal encoding strategies," *IEEE Transactions on Information Theory*, vol. 52, no. 22, pp. 5406–5424, 2006.

[5] A. M. Bruckstein, M. Elad, and M. Zibulevsky, "On the uniqueness of non-negative sparse and redundant representations," *ICASSP 2008, special session on Compressed Sensing, Las-Vegas, Nevada*, March, 2008.

[6] S.Foucart and M.-J. Lai, "Sparsest solutions of underdetermined linear systems via ℓ_q-minimization for $0 < q \leq 1$," *Applied and Computational Harmonic Analysis*, vol. 26, no. 3, pp. 395–407, 2009.

[7] Y. C. Pati, R. Rezahfar, and P.S. Krishnaprasad, "Orthogonal matching pursuit: Recursive function approximation with applications to wavelet decomposition," *Proc. 27th Asilomar Conference*, Los Alamitos, CA, USA, 2003.

[8] J. Bioucas-Dias and M. Figueiredo, "Alternating direction optimization for $\ell_2 - \ell_1$ problems in hyperspectral unmixing using," *2nd IEEE GRSS Workshop on Hyperspectral Image and Signal Processing - WHISPERS'2010*, 2010, submitted.

[9] S. Mallat and Z. Zhang, "Matching pursuits with time-frequency dictionaries," *IEEE Transactions on Signal Processing*, vol. 41, pp. 3397–3415, 1993.

[10] J. Eckstein and D. Bertsekas, "On the douglasrachford splitting method and the proximal point algorithm for maximal monotone operations," *Mathematical Programming*, vol. 5, pp. 293–318, 1992.

[11] M. Afonso, J. Bioucas-Dias, and M. Figueredo, "Fast image recovery using variable splitting and constrained optimization," *submitted to IEEE Transactions on Image Processing*, 2010.

[12] A. M. Bruckstein, D. L. Donoho, and M. Elad, "From sparse solutions of systems of equations to sparse modeling of signals and images," *SIAM Review*, vol. 51, pp. 34–81, 2009.